

The approximation of  $sp^3$  hybrids is obtained by setting  $d=0$ . In this case, we have  $\xi = \frac{3}{4}$  and  $\eta = 1$ . The fact that the  $sp^3$ -hybrids approach is a poor approximation is illustrated by noting that this pre-

dicts  $B_{xy}(0, 0, 4)$  to be zero when, in fact, it is large (see Table III). [It was noted by Feher<sup>4</sup> that  $d$  character was needed to explain  $B_{xy}(0, 0, 4)$ .]

\*Work supported in part by Army Research Office and National Science Foundation.

†Present address: Department of Physics, University of Missouri-Rolla, Rolla, Mo.

<sup>1</sup>J. M. Luttinger and W. Kohn, Phys. Rev. **97**, 869 (1955).

<sup>2</sup>W. Kohn and J. M. Luttinger, Phys. Rev. **98**, 915 (1955).

<sup>3</sup>W. Kohn, in *Solid State Physics*, edited by F. Seitz and D. Turnbull (Academic, New York, 1957), Vol. 5.

<sup>4</sup>G. Feher, Phys. Rev. **114**, 1219 (1959).

<sup>5</sup>E. B. Hale and R. L. Mieher, Phys. Rev. **184**, 739 (1969).

<sup>6</sup>E. B. Hale and R. L. Mieher, Phys. Rev. **184**, 751 (1969).

<sup>7</sup>A preliminary account of this work has appeared in E. B. Hale and R. L. Mieher, Phys. Letters **29A**, 350 (1969).

<sup>8</sup>G. G. Hall, Phil. Mag. **43**, 338 (1952); Proc. Phys. Soc. (London) **A66**, 1162 (1953).

<sup>9</sup>G. G. Hall, Phys. Rev. **90**, 317 (1953); Phil. Mag. **3**, 429 (1958).

<sup>10</sup>The values used for these constants in the numerical calculations were  $a_1 = 14.2 \text{ \AA}$ ,  $a_t = 25.0 \text{ \AA}$ ,  $a^* = 21.0 \text{ \AA}$ ,  $n(\text{As}) = 0.736$ ,  $n(\text{P}) = 0.800$ , and  $n(\text{Sb}) = 0.826$ . Various calculations using the envelope function in Eq. (2) have been discussed in Ref. 6.

<sup>11</sup>J. C. Slater and G. F. Koster, Phys. Rev. **94**, 1498 (1954).

<sup>12</sup>F. Herman, Phys. Rev. **88**, 1210 (1952).

<sup>13</sup>L. B. Redei, Proc. Roy. Soc. (London) **A270**, 373 (1962); **A270**, 383 (1962); D. Stocker, *ibid.* **A270**, 397 (1962); J. A. R. Coope, Ph. D. thesis, Oxford University,

1956 (unpublished), cited in above references; and N. V. Cohan, D. Pugh, and R. H. Tredgold, Proc. Phys. Soc. (London) **82**, 65 (1963).

<sup>14</sup>In Refs. 8 and 9, Hall used a fitting procedure to obtain expressions for the band energies along the symmetry directions. This procedure has also been used by D. L. Spears, M. A. thesis, Dartmouth College, 1964 (unpublished).

<sup>15</sup>W. A. Harrison, *Pseudopotentials in the Theory of Metals* (Benjamin, New York, 1966), and references cited therein.

<sup>16</sup>G. Dresselhaus and M. S. Dresselhaus, Phys. Rev. **160**, 649 (1967).

<sup>17</sup>P. W. Anderson, Phys. Rev. Letters **21**, 13 (1968).

<sup>18</sup>These calculations are discussed in detail in E. B. Hale, Ph. D. thesis, Purdue University, 1968 (unpublished).

<sup>19</sup>J. L. Ivey and R. L. Mieher (unpublished).

<sup>20</sup>The available data on the location of  $k_0$  are discussed in detail by E. B. Hale and T. G. Castner, Jr., Phys. Rev. B **1**, 4763 (1970).

<sup>21</sup>One check on our formulation of the wave function in terms of equivalent orbitals is that we obtain the same expression for the contact interaction that is discussed in Refs. 4 and 6.

<sup>22</sup>A recent improvement [R. A. Faulkner, Phys. Rev. **184**, 713 (1969)] in the effective-mass approach has yielded accurate values for the energies of the excited states of the shallow donors. However, the problems of the ground-state wave functions and energies are related to the "chemical-shift" phenomenon and are not related to the approximations in the solution of the effective-mass Hamiltonian.

## Longitudinal Optical Phonons in Thin Films of CdS, CdSe, and Their Mixtures

G. Lubberts\*

*Department of Electrical Engineering, University of Rochester, Rochester, New York 14627*

(Received 28 September 1970)

LO phonon energies have been determined by means of electron tunneling in Sn-SnO-semiconductor-Sn junctions. For mixtures of CdS and CdSe, we find two distinct structures in the tunneling data which occur at lower energies than the LO phonons for pure CdS and CdSe. These results agree with infrared spectroscopic data on bulk crystals. This agreement provides strong evidence that only short-range forces are important in determining the optical-phonon spectra.

In recent experiments, Giaever and Zeller<sup>1-3</sup> as well as MacVicar *et al.*,<sup>4</sup> have demonstrated that it is possible for electrons to tunnel through thin layers of semiconducting materials which are sandwiched between two metal films. By examining the current-voltage ( $I$ - $V$ ) curve of such tunneling junctions, Giaever and Zeller<sup>2,3</sup> found a resistance de-

crease in such devices at applied voltages corresponding to the longitudinal optical (LO) phonon energy of the semiconductor material. Such resistance changes are usually observable when first- or second-derivative measurements are made of the  $I$ - $V$  curve. The decrease in resistance can be explained by considering the interaction of the tun-

neling electron with a LO phonon in the barrier. In such an interaction the electron suffers an energy loss equal to the phonon energy. Such an inelastic tunneling process causes a new tunneling channel to open up at applied voltages equal to or greater than the LO phonon energy. The creation of an additional tunneling channel will give rise to a decrease in the dynamic resistance of the tunnel junction. Such a tunneling process is analogous to the interaction of the tunneling electron with vibrational modes of foreign molecules adsorbed to the barrier of a tunnel junction.<sup>5</sup>

CdS and some other II-VI compound films as tunneling barriers have been examined by Giaever and Zeller<sup>1-3</sup> and our result for CdS concerning the LO phonon structure in the  $I-V$  characteristic is in agreement with their data. In addition to CdS tunneling barriers, we have investigated CdSe barriers, as well as mixtures of CdS and CdSe. We find that barriers consisting of mixtures of CdS and CdSe give two distinct phonon structures in the tunneling data. The energies of these two LO phonons are slightly lower than those for pure CdS and CdSe. The occurrence of these two bands has also been found in infrared reflectance data for single crystals of CdS/CdSe.<sup>6</sup> We interpret these results as strong evidence that only short-range forces are important in determining the optical-phonon spectra.

In all our junctions, we used tin (Sn) for both metal electrodes. The tunneling structures were made in the following manner: First a metallic film of Sn was deposited on a sapphire substrate by evaporating Sn at a pressure of about  $1.0 \times 10^{-6}$  mm of Hg. Subsequently, a thin oxide film was grown on the Sn film by means of a glow discharge technique.<sup>7</sup> Pure oxygen gas was introduced into the bell jar for the glow discharge procedure. The next step in the junction fabrication process was to evaporate a thin film of semiconducting material. The CdS/CdSe mixed films were obtained by simultaneously evaporating CdS and CdSe. The pressure in the bell jar during the semiconductor evaporations was less than  $7.0 \times 10^{-6}$  mm of Hg. The junctions were completed by depositing a Sn film as counter electrode. The two electrodes crossed each other at right angles so that four probe measurements could be made. At no time during the junction fabrication process was the specimen exposed to room air.

During the semiconductor evaporation and the oxidation process, the substrate was kept at 25 °C while for the Sn evaporations, the substrate was kept at about -20 °C. This low substrate temperature improved edge sharpness of the metal films. The size of our junctions was  $0.22 \times 0.41$  mm ( $0.09$  mm<sup>2</sup>). The semiconductor thickness of the junctions ranged from 75 to 150 Å.

Since thin evaporated semiconductor layers are usually not continuous, one might expect some of the tunneling current to flow through the tin oxide areas of pinhole size not covered with a semiconductor layer. As we shall see presently, the prominent LO phonon structure in the  $I-V$  curve is clear evidence that a substantial fraction of the tunneling current flows through the semiconductor layer. Also, the asymmetrical nature of the  $I-V$  curve corroborates this conclusion. When electrons tunnel through the oxide as well as the semiconductor layer, we expect an asymmetrical  $I-V$  curve since we have an asymmetrical junction.

The asymmetry in the  $I-V$  curve is demonstrated in Fig. 1, where the dynamic resistance  $dV/dI$  is plotted as a function of voltage  $V$  for three semiconductor barriers.<sup>8</sup> The asymmetry occurs even though the oxide thickness is much smaller than the semiconductor thickness. Typically, we obtain a resistance of only  $0.05 \Omega$  for Sn-SnO-Sn junctions at 1.4 °K (obtained by deleting the semiconductor layer). These junctions give a dc Josephson current of several mA and consequently the thickness of the oxide layers is less than 10 Å. We note that when these junctions were cooled to 1.4 °K we usually ob-

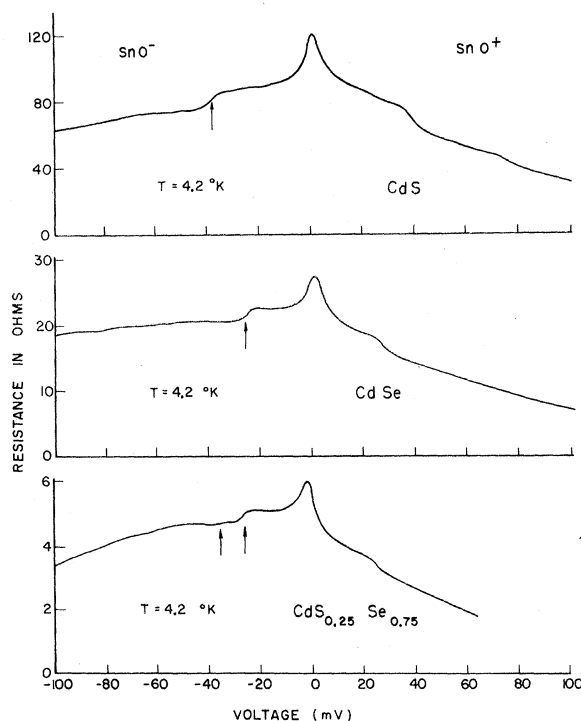


FIG. 1. Dynamic resistance  $dV/dI$  as a function of voltage for three tunnel junctions of the type Sn-SnO-X-Sn where X denotes CdS, CdSe, or  $\text{CdS}_{0.25}\text{Se}_{0.75}$ . The designation  $\text{SnO}^+$  means that the metal electrode adjacent to the SnO layer is at a positive potential relative to the other metal electrode. The LO phonon structures are indicated by arrows for the  $\text{SnO}^-$  polarity.

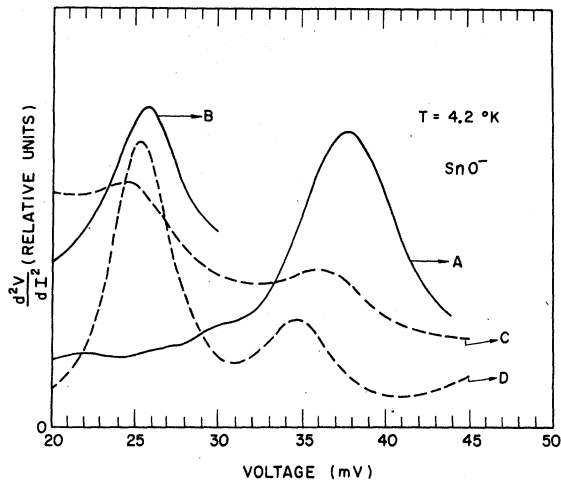


FIG. 2.  $d^2V/dI^2$  as a function of voltage for tunnel junctions with four different semiconductor barriers: (A) CdS; (B) CdSe; (C)  $\text{CdS}_{0.47}\text{Se}_{0.53}$ ; (D)  $\text{CdS}_{0.25}\text{Se}_{0.75}$ .

tained an almost ideal single-particle tunneling characteristic. By almost ideal we mean that the ratio of currents corresponding to the voltages  $0.9 (2\Delta/e)$  and  $1.1 (2\Delta/e)$  is typically 0.01. The term  $2\Delta$  refers to the superconducting energy gap, and  $e$  is the electronic charge. Using the same criterion for our semiconductor junctions, we get a current ratio between 0.06 and 0.2 at  $1.4^\circ\text{K}$ , depending on the junction. This implies that the major portion of the electrons tunnel directly from one metal electrode to the other in a one-step process.

In Fig. 1 one notes sudden decreases in resistance which occur in the voltage range 25–40 mV. Such decreases in resistance are attributed to the interaction of the tunneling electrons with the LO phonons of the semiconductor barrier. For the CdS and CdSe barriers, even two-phonon events occurring at twice the LO phonon energy are observable in the original data and can be identified when second-derivative measurements are made of the  $I$ - $V$  curve. By taking second-derivative data, we find that the center of the LO phonon energy band occurs at 38 meV for CdS and 26 meV for CdSe. We note that for the  $\text{SnO}^-$  polarity (see Fig. 1) the background resistance is nearly constant in the voltage region where the LO phonon structures occur. Hence, for the  $\text{SnO}^-$  polarity, we have an almost ideal situation for measuring LO phonon structures. The specific cause of the resistance increase around zero bias is not known but is often found in tunneling junctions.

By examining the second derivative  $d^2V/dI^2$  as a function of  $V$  for mixed crystal barriers, we find two LO phonon bands corresponding to the CdSe and CdS components. In Fig. 2, we show  $d^2V/dI^2$  versus  $V$  over the voltage range of interest. This figure shows that as the CdSe concentration is increased in the mixture, the LO phonon energy corresponding

to the CdS decreases. For example, we find that for a  $\text{CdS}_{0.25}\text{Se}_{0.75}$  barrier the LO phonon energy peak corresponding to the CdS component has decreased 3 meV relative to that of the CdS barrier, while for a  $\text{CdS}_{0.47}\text{Se}_{0.53}$  barrier the CdS LO phonon energy peak has decreased 2 meV relative to that of the CdS barrier. On the other hand, the decrease in phonon energy for the CdSe component is about 1 meV for the  $\text{CdS}_{0.47}\text{Se}_{0.53}$  barrier. The appearance of two distinct LO phonon structures as well as the magnitude of the shift in the phonon energy is in agreement with infrared spectroscopic data for bulk crystals of CdS/CdSe.<sup>6</sup> (We have attempted to cause a shift in the CdSe component larger than that shown in Fig. 2 by increasing the percentage of CdS in the mixture. However, the technique for preparing junctions described in this paper yielded samples with a very nonlinear  $I$ - $V$  curve when the mole fraction of CdS began to exceed that of CdSe. That is, the resistance decreased rapidly in the voltage range 0–40 mV. This means that relatively small resistance decreases due to LO phonon-electron interactions become difficult to detect when superimposed on a rapidly decreasing background resistance.)

CdS films of about  $1 \mu$  thickness were evaporated directly on the substrate to investigate some properties of our semiconductor barriers. Hall-effect and resistivity measurements performed on such a sample at room temperature revealed a very high donor concentration ( $N_D > 1.5 \times 10^{19}/\text{cm}^3$ ). The high donor concentration implies that such samples have a large excess of cadmium or a large number of sulfur vacancies. Undoubtedly many other types of defects are present in our barrier layers.<sup>9</sup>

On the basis of the large number of imperfections in our semiconductor barriers, interactions between atoms are essentially limited to nearest neighbors. Thus, at first sight it might be surprising to find such good agreement between our tunneling results and infrared spectroscopic data on well-defined single crystals.<sup>6</sup> However, the occurrence of two phonon bands in structurally well-defined mixed crystals of CdS/CdSe has been explained as resulting from a crystal system where short-range forces are dominant.<sup>10</sup> The fact that two LO phonon bands are also found by electron tunneling through films where *only* short-range order exists gives strong experimental support to this view. Thus, our LO phonon data for CdS, CdSe, and particularly their mixtures provide evidence beyond Giaever and Zeller's results<sup>2,3</sup> that only short-range order is of importance in determining the optical-phonon spectra.

The author gratefully acknowledges helpful discussions with Dr. D. L. Losee of the Kodak Research Laboratories. Also, the author is indebted to Professor S. Shapiro of the University of Rochester for his advice and his interest in this work.

\*Supported by a Doctoral Award from Eastman Kodak Company.

<sup>1</sup>I. Giaever, Phys. Rev. Letters 20, 1286 (1968).

<sup>2</sup>I. Giaever and H. R. Zeller, J. Vac. Sci. Technol. 6, 502 (1969).

<sup>3</sup>I. Giaever and H. R. Zeller, Phys. Rev. Letters 21, 1385 (1968).

<sup>4</sup>M. L. A. MacVicar, S. M. Freake, and C. J. Adkins, J. Vac. Sci. Technol. 6, 717 (1969).

<sup>5</sup>R. C. Jaklevic and J. Lambe, Phys. Rev. Letters 17, 1139 (1966).

<sup>6</sup>J. F. Parrish, C. H. Perry, O. Brafman, I. F. Chang, and S. S. Mitra, in *II-VI Semiconducting*

*Compounds*, edited by D. G. Thomas (Benjamin, New York, 1967), p. 1164; M. Balkanski, *ibid.*, p. 1007.

<sup>7</sup>J. L. Miles and P. H. Smith, J. Electrochem. Soc. 110, 1240 (1963).

<sup>8</sup>First- and second-derivative measurements were made using standard modulation techniques. Our circuitry was patterned after a design by A. Longacre, Jr. [Rev. Sci. Instr. 41, 448 (1970)].

<sup>9</sup>K. L. Chopra, *Thin Film Phenomena* (McGraw-Hill, New York, 1969), Chap. IV.

<sup>10</sup>M. Balkanski, R. Beserman, and J. M. Besson, Solid State Commun. 4, 201 (1966).

## Second-Order Raman Spectrum of MgO†

N. B. Manson,\* W. Von der Ohe, and S. L. Chodos

*Department of Physics, University of California, Los Angeles, California 90024*

(Received 17 August 1970)

The second-order Raman spectrum of MgO at room temperature is reported for different polarizations and crystal orientations. The parts of the scattering polarizability transforming as  $A_{1g}$ ,  $E_g$ , and  $T_{2g}$  are separated and compared with features in the two-phonon dispersion curves at the critical points  $\Gamma$ ,  $X$ ,  $L$ , and  $W$ .

### INTRODUCTION

The lattice dynamics of MgO has been the subject of extensive experimental and theoretical investigations as can be seen from the numerous publications on the subject. These have included studies of neutron scattering,<sup>1,2</sup> infrared absorption,<sup>3,4</sup> and vibronic transitions of impurity ions.<sup>5-8</sup> However, there is a lack of reliable Raman data - those reported previously being in error<sup>9</sup> or incomplete.<sup>10</sup>

MgO has the rocksalt structure and hence shows no first-order Raman effect. The second-order spectrum has been clearly identified, and is reported here for different polarizations and crystal orientations. The strong features are considered to arise from points of high density of states near critical points in the Brillouin zone and, therefore, comparison is made to the two-phonon dispersion curves which have been constructed with the help of neutron data.<sup>1,2</sup>

### EXPERIMENTAL

The exciting source was a Spectra Physics model 141 argon ion laser, which gave a multimode power of 300 mW in the 4880-Å line. The beam was focused on the crystal with a 3-cm-focal-length lens. An  $f/1.5$  cone of light scattered at right angles was collected and dispersed by a Spex 1401 double monochromator. It was detected by a cooled ITT FW 130 photomultiplier using photoncounting techniques. The incident beam passed through a narrow bandpass interference filter in order to

keep the nonlasing  $A^+$  lines from distorting the spectra, and then through a double Fresnel rhomb. With the latter device the direction of polarization of the incoming beam could be rotated by 90°. The scattered beam was analyzed by a Polaroid sheet placed in front of the entrance slit. The final scans were recorded at a speed of 3 Å/min with a 5-sec time constant and a spectral slitwidth of 8  $\text{cm}^{-1}$ .

Initially spectra were taken of six different MgO crystals and with three different laser lines. Two of the crystals were deliberately doped, the remaining four not. However, these crystals had all been grown in an electric arc furnace and are known to contain numerous kinds of impurities.<sup>11</sup> At least the coarse structure consisting of five broad peaks and one comparatively narrow one nearly at the center was observed in each case.

Two further phenomena were exhibited by every crystal and with every laser line: (i) The low-lying band peaked at 128  $\text{cm}^{-1}$ , and (ii) a fluorescent background. Both can be seen in Fig. 1.

The intensity of the low-energy band varies little from sample to sample. It is assumed to be a difference band and is under further investigation. The fluorescence background represents the short-wavelength side of a broad smooth emission band, which reaches its peak at around 6000 Å. Its intensity varies from sample to sample and also within one specimen from point to point. This emission is thought to be caused by some imperfection which is present in all crystals but whose concentration is not constant. The final spectra, which